Proceedings of the
Annual Stability Conference
Structural Stability Research Council
St. Louis, Missouri, April 2-5, 2019

Stiffness matrix for buckling analysis of tapered steel members

Emad S. Salem[1]

Abstract
Web tapered members are vastly used for steel structures. However, calculating their critical buckling loads involves applying numerical integration or charts or complicated equations. In an attempt to develop a simple, yet an accurate, solution for this problem, a closed form stiffness matrix for buckling analysis of web tapered steel member is proposed, which could be applied to a wide range of tapered steel structures. Moreover, with the advance in steel member design using "Direct Analysis Method", the critical buckling load of a column is considered with an effective buckling length equal to its unbraced length. Applying the closed form stiffness matrix, developed in this research, yields the critical buckling load for a column with any boundary conditions. Verification examples are provided to illustrate the accuracy of the procedures.

1. Introduction

There are four widely applied approaches to calculate the elastic critical buckling load of tapered steel members: (1) accurate analytical formulation of the stiffness matrix, (2) charts and tables, (3) numerical calculation of stiffness matrix, and (4) dividing the tapered member into adequate numbers of members with prismatic sections.

Bai et al. (2018) developed an analytical equation for calculating the stiffness matrix for different tapered sections using the tapered-variability indexes to represent the variations in the stiffness along the member. Liu et al. (2016) derived an analytical equation to represent the stiffness matrix of tapered members using series of stiffness factors. Simple and fast approximate procedures were proposed by Bazeos and Karabalis (2006), Williams and Aston (1989) and were presented in chart format. Numerical evaluation of stiffness matrix for tapered member was adopted by SAP 2000 (2009). Kaehler et al. (2011) applied the method of successive approximations (developed by Timoshenko and Gere (1961)) to calculate the critical buckling load of tapered member. Dividing the tapered member into segments of prismatic members was implemented by Funk and Wang (1988). Most of the previous approaches are either cumbersome to be implemented by steel designers or incorporated in a computer design program.

In this research, a simple, yet an accurate, method for formulating the stiffness matrix for buckling analysis of tapered steel members is presented. This method could be applied to a wide variety of web tapered columns, even if the column has two different tapered segments with

[1] Associate Professor , Al-Azhar University <emadsalem@azhar.edu.eg>

different flange and web thicknesses. As well as, it could be applied to a column with one tapered segment and the other segment is prismatic. The critical buckling load of stepped column with different axial load in each segment could be determined using the proposed procedures. For prismatic columns, the stiffness matrix of web tapered member will automatically yield that of a prismatic member and hence the procedures are equally applied to prismatic sections. Another benefit of developing a closed form stiffness matrix for buckling analysis of web tapered members is its application in a computerized program to determine the elastic critical buckling load.

2. Flexural Flexibility and Stiffness Matrices for Web Tapered Member

In this formulation, only the flexural deformation is considered: the axial and shear deformations are not considered. In order to formulate the flexural flexibility and stiffness matrices of web tapered member, the moment of inertia variation along the member is assumed as:

$$I(x) = [b - cx]^2 \tag{1}$$

where, $a = \sqrt{I_e}$, $b = \sqrt{I_s}$, $c = \dfrac{b-a}{L}$; I_s and I_e are the moments of inertia at start and end of the tapered member (Fig. 1), respectively; L is the member length; and $I(x)$ is the moment of inertia at distance x from the member start as shown in Fig. 1. Eq. 1 represents with sufficient accuracy the variation of moment of inertia along a tapered member with constant flange width and linearly varying web depth. This equation is a simplified form of that developed by SAP 2000 (2009) as shown in the verification manual.

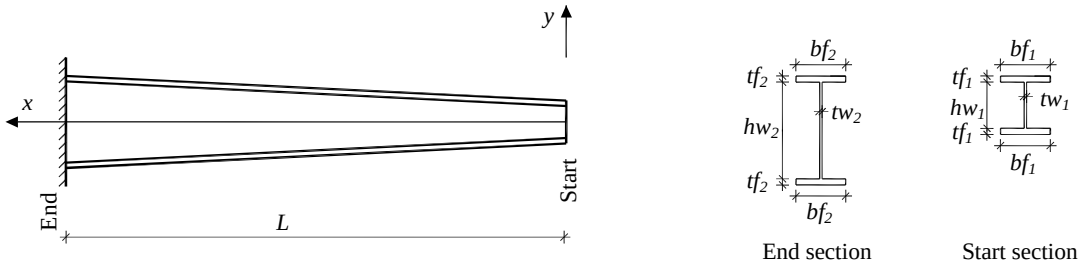

Figure 1: Tapered member geometry

The concept of equivalent moment of inertia will be used in deriving both the flexibility and stiffness matrices for a web tapered member. This concept is based on having the same deformation for both nonprismatic and its equivalent prismatic member under the same set of loads. The first column of the flexibility matrix (Eq. 2) is determined by applying a unit load as shown in Fig. 2a, where fv_{ij} = deformation at DOF i due to a unit load at DOF j with all other deformations unrestrained and all other forces equal to zero.

$$Fv = \begin{bmatrix} fv_{22} & fv_{23} \\ fv_{32} & fv_{33} \end{bmatrix} \tag{2}$$

From Fig. 2b, the bending moment variation due to a unit load can be expressed as:

$$M(x) = x \tag{3}$$

To calculate fv_{22} for nonprismatic member shown in Fig. 1, use Eq. 4. For its equivalent prismatic member, fv_{22} is calculated using Eq. 5 (in all calculations the bending moments shown in Fig. 2b are used).

$$(fv_{22})_{nonprismatic} = \int_0^L \frac{M_0 M_1}{EI(x)} dx = \frac{1}{E} \int_0^L \frac{[M(x)]^2}{I(x)} dx = \frac{1}{E} \int_0^L \frac{x^2}{[b-cx]^2} dx \tag{4}$$

$$(fv_{22})_{prismatic} = \int_0^L \frac{M_0 M_1}{EI_1} dx = \frac{1}{EI_1} \int_0^L [M(x)]^2 dx = \frac{1}{EI_1} \int_0^L x^2 dx \tag{5}$$

where E is the modulus of elasticity, L is the member length, $M(x)$ is the bending moment at distance x from the member start, and I_1 is the moment of inertia of the equivalent prismatic member (for calculating fv_{22}).

By imposing the condition that the deformations fv_{22} for both nonprismatic (Eq. 4) and its equivalent prismatic member (Eq. 5) are equal, yields:

$$\frac{1}{I_1} \int_0^L x^2 dx = \int_0^L \frac{x^2}{[b-cx]^2} dx \tag{6}$$

The integration and simplification of Eq. 6 result in:

$$I_1 = \frac{(b-a)^2}{3\left[1 + \frac{b}{a} + \frac{2b}{(b-a)} Ln\left(\frac{a}{b}\right)\right]} \tag{7}$$

where Ln is the natural logarithm. Eq. 7 maps a web tapered member (with constant flange width and varying web depth) to a prismatic one with an equivalent moment of inertia, I_1. Note that in Eq. 7 as constant a approaches b (for a prismatic member), I_1 becomes infinite. However, by applying the limit to Eq. 7, it can be shown that I_1 approaches b^2. Therefore:

$$(fv_{22})_{nonprismatic} = \frac{1}{EI_1} \int_0^L x^2 dx = \frac{L^3}{3EI_1} \tag{8}$$

To calculate fv_{32} for nonprismatic member shown in Fig. 1, use Eq. 9. For its equivalent prismatic member, fv_{32} is calculated using Eq. 10 (in all calculations the bending moments shown in Fig. 2c are used).

$$(fv_{32})_{nonprismatic} = \int_0^L \frac{M_0 M_2}{EI(x)} dx = \frac{1}{E} \int_0^L \frac{M(x)}{I(x)} dx = \frac{1}{E} \int_0^L \frac{x}{[b-cx]^2} dx \tag{9}$$

$$(fv_{32})_{prismatic} = \int_0^L \frac{M_0 M_2}{EI_2} dx = \frac{1}{EI_2} \int_0^L M(x) dx = \frac{1}{EI_2} \int_0^L x dx \tag{10}$$

where I_2 is the moment of inertia of the equivalent prismatic member (for calculating fv_{32}).

By imposing the condition that the deformations fv_{32} for both nonprismatic (Eq. 9) and its equivalent prismatic member (Eq. 10) are equal, yields:

$$\frac{1}{I_2} \int_0^L x dx = \int_0^L \frac{x}{[b - cx]^2} dx \tag{11}$$

The integration and simplification of Eq. 11 result in:

$$I_2 = \frac{(b-a)^2}{2\left[Ln\left(\frac{a}{b}\right) + \frac{b}{a} - 1 \right]} \tag{12}$$

Note that in Eq. 12 as constant a approaches b (for a prismatic member), I_2 becomes zero. However, by applying the limit to Eq. 12, it can be shown that I_2 approaches b^2. Therefore:

$$(fv_{32})_{nonprismatic} = \frac{1}{EI_2} \int_0^L x dx = \frac{L^2}{2EI_2} \tag{13}$$

Now the first column of flexibility matrix has been formed.

To calculate fv_{33} for nonprismatic member shown in Fig. 1, use Eq. 14. For its equivalent prismatic member, fv_{33} is calculated using Eq. 15 (in all calculations the bending moments shown in Fig. 2-d are used).

$$(fv_{33})_{nonprismatic} = \int_0^L \frac{(M_2)^2}{EI(x)} dx = \frac{1}{E} \int_0^L \frac{1}{I(x)} dx = \frac{1}{E} \int_0^L \frac{1}{[b - cx]^2} dx \tag{14}$$

$$(fv_{33})_{prismatic} = \int_0^L \frac{(M_2)^2}{EI_3} dx = \frac{1}{EI_3} \int_0^L dx \tag{15}$$

where I_3 is the moment of inertia of the equivalent prismatic member (for calculating fv_{33}).

By imposing the condition that the deformations fv_{33} for both nonprismatic (Eq. 14) and its equivalent prismatic member (Eq. 15) are equal, yields:

$$\frac{1}{I_3} \int_0^L dx = \int_0^L \frac{1}{[b - cx]^2} dx \tag{16}$$

The integration and simplification of Eq. 16 result in:

$$I_3 = ab \tag{17}$$

$$(fv_{33})_{nonprismatic} = \frac{1}{EI_3}\int_0^L dx = \frac{L}{EI_3} \tag{18}$$

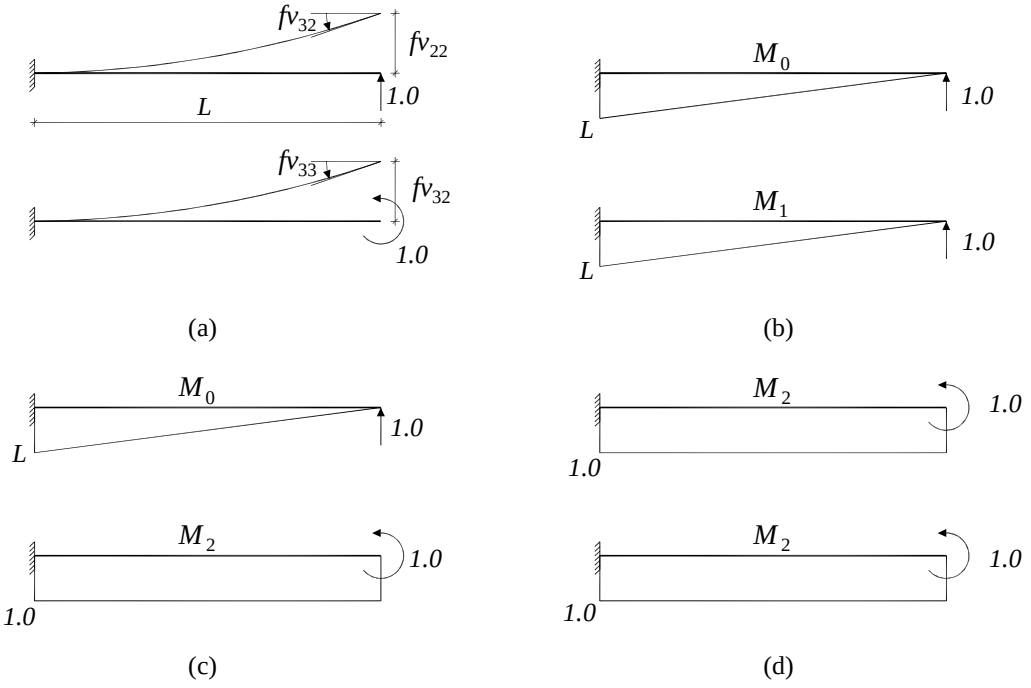

Figure 2: Flexibility coefficients

The flexibility matrix of nonprismatic cantilever member in terms of its equivalent prismatic member can be expressed as:

$$Fv_{(nonprismatic)} = \frac{L}{E}\begin{bmatrix} \frac{L^2}{3I_1} & \frac{L}{2I_2} \\ \frac{L}{2I_2} & \frac{1}{I_3} \end{bmatrix} \tag{19}$$

For a prismatic member, where $a = b$, the limit of Eqs. 7 and 12; and Eq. 17 yields:

$$I_1 = I_2 = I_3 = I = a^2 = b^2 \tag{20}$$

The inverse of flexibility matrix, Eq. 19, yields the flexural stiffness matrix for nonprismatic cantilever member, $k_{nonprismatic}$, as:

$$k_{nonprismatic} = d\begin{bmatrix} \frac{L}{EI_3} & \frac{-L^2}{2EI_2} \\ \frac{-L^2}{2EI_2} & \frac{L^3}{3EI_1} \end{bmatrix} \tag{21}$$

where

$$d = \frac{12E^2}{L^4\left(\frac{4}{I_1 I_3} - \frac{3}{I_2^2}\right)} \tag{22}$$

For a prismatic cantilever member, where $I_1 = I_2 = I_3 = I$, the flexural stiffness matrix in Eq. 21 yields:

$$k_{prismatic} = \begin{bmatrix} \frac{12EI}{L^3} & \frac{-6EI}{L^2} \\ \frac{-6EI}{L^2} & \frac{4EI}{L} \end{bmatrix} \tag{23}$$

The nonprismatic flexural stiffness matrix (Eq. 21) of a cantilever member (Fig. 3-a) can be transformed to local member coordinates (Fig. 3-c) as follows:

.

$$k_{nonprismatic} = \begin{bmatrix} -1 & 0 \\ -L & -1 \\ 1 & 0 \\ 0 & 1 \end{bmatrix} d \overset{\begin{matrix} h_1 & h_2 \end{matrix}}{\begin{bmatrix} \frac{L}{EI_3} & \frac{-L^2}{2EI_2} \\ \frac{-L^2}{2EI_2} & \frac{L^3}{3EI_1} \end{bmatrix}} \begin{bmatrix} -1 & -L & 1 & 0 \\ 0 & -1 & 0 & 1 \end{bmatrix} \tag{24}$$

$$k_{nonprismatic} = \frac{d.L}{E} \overset{\begin{matrix} d_1 & d_2 & d_3 & d_4 \end{matrix}}{\begin{bmatrix} \frac{1}{I_2} & \left(\frac{L}{I_2} - \frac{L}{2I_3}\right) & \frac{-1}{I_2} & \frac{L}{2I_3} \\ \left(\frac{L}{I_2} - \frac{L}{2I_3}\right) & \left(\frac{L^2}{3I_1} + \frac{L^2}{I_2} - \frac{L^2}{I_3}\right) & -\left(\frac{L}{I_2} - \frac{L}{2I_3}\right) & -\left(\frac{L^2}{3I_1} - \frac{L^2}{2I_3}\right) \\ \frac{-1}{I_2} & -\left(\frac{L}{I_2} - \frac{L}{2I_3}\right) & \frac{1}{I_2} & \frac{-L}{2I_3} \\ \frac{L}{2I_3} & -\left(\frac{L^2}{3I_1} - \frac{L^2}{2I_3}\right) & \frac{-L}{2I_3} & \frac{L^2}{3I_1} \end{bmatrix}} \tag{25}$$

where, h_1 and h_2 are the vertical displacement and rotation of the cantilever member (Fig 3-b), respectively. In local member coordinates, d_1, d_2 , d_3 , and d_4 are the vertical displacement and rotation at the end and start of the member, respectively, as shown in Fig. 3-c.

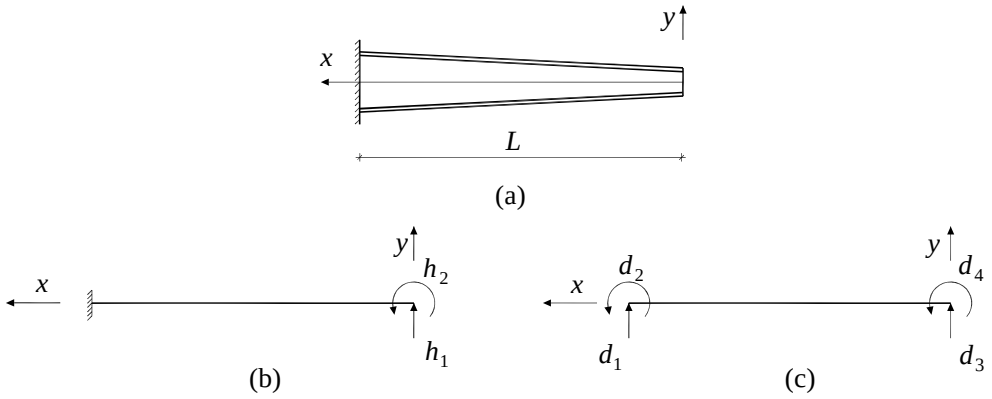

Figure 3: Stiffness matrix transformation: (a) tapered cantilever member, (b) cantilever DOF, (c) DOF in local coordinates

3. Geometric Stiffness Matrix for Web Tapered Member

The geometric stiffness of a member includes both *P*-δ and *P*-**D** effects. The *P*-δ effect arises from member flexure while *P*-**D** arises from chord rotation as shown in Fig. 4. As a result, the effect of *P*-**D** will be the same for both prismatic and nonprismatic members. However, the effect of *P*-δ will not be the same for both prismatic and nonprismatic members. Since the effect of *P*-**D** dominates the behavior of the member (Teh 2001), the geometric stiffness matrix for nonprismatic member, for simplicity, is taken equal to that of a prismatic one. The geometric stiffness for a prismatic member is given by Cook et al. (1989) (Eq. 26). To reduce the error resulting from this simplification, the member is divided into two elements as shown in Fig. 5. The geometric stiffness matrix, k_G, for a web tapered member subjected to axial compression can be expressed in local member coordinates as:

$$k_G = \frac{-P}{30L}\begin{array}{c} \begin{matrix} d_1 & d_2 & d_3 & d_4 \end{matrix} \\ \begin{bmatrix} 36 & 3L & -36 & 3L \\ 3L & 4L^2 & -3L & -L^2 \\ -36 & -3L & 36 & -3L \\ 3L & -L^2 & -3L & 4L^2 \end{bmatrix} \end{array} \tag{26}$$

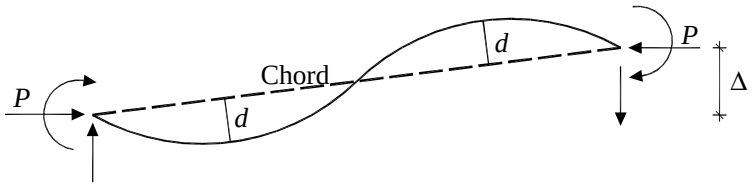

Figure 4: P-δ and P-**D** effects

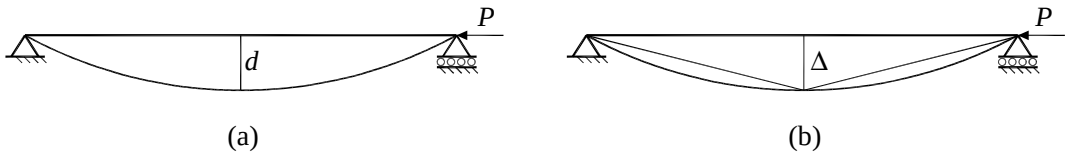

Figure 5: Effect of P-δ and P-$\mathbf{D}$: (a) one element per member , (b) two elements per member

4. Elastic Critical Buckling Load

The elastic critical buckling load of web tapered column is calculated using eigenvalue technique. For each member, the flexural and geometric stiffness matrices are formed using Eqs. 27 and 28, where the subscript i refers to the member number.

$$k_i = \begin{array}{c} \begin{matrix} d_1 & d_2 & d_3 & d_4 \end{matrix} \\ \begin{bmatrix} (k_{11})_i & (k_{12})_i & (k_{13})_i & (k_{14})_i \\ (k_{21})_i & (k_{22})_i & (k_{23})_i & (k_{24})_i \\ (k_{31})_i & (k_{32})_i & (k_{33})_i & (k_{34})_i \\ (k_{41})_i & (k_{42})_i & (k_{43})_i & (k_{44})_i \end{bmatrix} \end{array} \tag{27}$$

$$k_{Gi} = \begin{array}{c} \begin{matrix} d_1 & d_2 & d_3 & d_4 \end{matrix} \\ \begin{bmatrix} (k_{G11})_i & (k_{G12})_i & (k_{G13})_i & (k_{G14})_i \\ (k_{G21})_i & (k_{G22})_i & (k_{G23})_i & (k_{G24})_i \\ (k_{G31})_i & (k_{G32})_i & (k_{G33})_i & (k_{G34})_i \\ (k_{G41})_i & (k_{G42})_i & (k_{G43})_i & (k_{G44})_i \end{bmatrix} \end{array} \tag{28}$$

Each element in the stiffness matrices of Eqs. 27 and 28 is calculated using Eqs. 25 and 26, respectively. For example:

$$(k_{11})_1 = \frac{d_1 L_1}{E(I_2)_1} \quad \text{and} \quad (k_{G11})_1 = \frac{-6P_1}{5L_1} \tag{29}$$

The flexural stiffness matrix, $[K]$, for the entire structure will be obtained by transforming the individual element stiffness matrices from element to structure coordinate and then combining the resulting matrices. For example; $[K]$ for a column consists of two elements (as shown in Fig. 6) is given by Eq. 30. Similarly, the geometric stiffness for the entire structure, $[K_G]$, is formed. The flexural stiffness matrix, given by Eq. 30, is valid for any boundary conditions. For a simply supported column shown in Fig. 6-b, the displacement at the start and end of the column is zero ($\Delta_1 = \Delta_5 = 0$). Eliminating the columns and rows corresponding to Δ_1 *and* Δ_5 yields the flexural stiffness matrix for a simply supported column (Eq. 31). Similarly, the geometric stiffness matrix for a simply supported column is given by Eq. 32.

$$[K]=\begin{array}{c}\begin{matrix}\Delta_1 & \Delta_2 & \Delta_3 & \Delta_4 & \Delta_5 & \Delta_6\end{matrix}\\ \begin{bmatrix}(k_{11})_1 & (k_{12})_1 & (k_{13})_1 & (k_{14})_1 & 0 & 0\\ (k_{21})_1 & (k_{22})_1 & (k_{23})_1 & (k_{24})_1 & 0 & 0\\ (k_{31})_1 & (k_{32})_1 & (k_{33})_1+(k_{11})_2 & (k_{34})_1+(k_{12})_2 & (k_{13})_2 & (k_{14})_2\\ (k_{41})_1 & (k_{42})_1 & (k_{43})_1+(k_{21})_2 & (k_{44})_1+(k_{22})_2 & (k_{23})_2 & (k_{24})_2\\ 0 & 0 & (k_{31})_2 & (k_{32})_2 & (k_{33})_2 & (k_{34})_2\\ 0 & 0 & (k_{41})_2 & (k_{42})_2 & (k_{43})_2 & (k_{44})_2\end{bmatrix}\end{array} \tag{30}$$

$$[K]=\begin{array}{c}\begin{matrix}\Delta_2 & \Delta_3 & \Delta_4 & \Delta_6\end{matrix}\\ \begin{bmatrix}(k_{22})_1 & (k_{23})_1 & (k_{24})_1 & 0\\ (k_{32})_1 & (k_{33})_1+(k_{11})_2 & (k_{34})_1+(k_{12})_2 & (k_{14})_2\\ (k_{42})_1 & (k_{43})_1+(k_{21})_2 & (k_{44})_1+(k_{22})_2 & (k_{24})_2\\ 0 & (k_{41})_2 & (k_{42})_2 & (k_{44})_2\end{bmatrix}\end{array} \tag{31}$$

$$[K_G]=\begin{array}{c}\begin{matrix}\Delta_2 & \Delta_3 & \Delta_4 & \Delta_6\end{matrix}\\ \begin{bmatrix}(k_{G22})_1 & (k_{G23})_1 & (k_{G24})_1 & 0\\ (k_{G32})_1 & (k_{G33})_1+(k_{G11})_2 & (k_{G34})_1+(k_{G12})_2 & (k_{G14})_2\\ (k_{G42})_1 & (k_{G43})_1+(k_{G21})_2 & (k_{G44})_1+(k_{G22})_2 & (k_{G24})_2\\ 0 & (k_{G41})_2 & (k_{G42})_2 & (k_{G44})_2\end{bmatrix}\end{array} \tag{32}$$

For calculating the elastic critical buckling load, the global stiffness equation is expressed in the form of eigenvalue problem (McGuire et al. (2000)) in which the equilibrium equation at the buckling is:

$$[[K]+l[K_G]]\{\Delta\}=\{0\} \tag{33}$$

where l (an eigenvalue) is the load vector with respect to a reference load $\{P\}$, and $\{\Delta\}$ (an eigenvector) is the buckled shape. The lowest value of $l\{P\}$ that satisfies Eq. 33 for $\{\Delta\}\neq 0$ yields the elastic critical buckling load $l\{P\}$, and the corresponding $\{\Delta\}$ defines the buckled shape.

5. Verification Examples

To demonstrate the efficiency and accuracy of the proposed method, several examples are analyzed and compared with analytical and numerical solutions available in the literature. Only bending stiffness was considered in the proposed method: the axial and shear stiffnesses were not considered.

5.1 Example 1

A cantilever linearly tapered steel column I-section, shown in Fig. 6-a, with modulus of elasticity E = 206.85 GPa and height L = 254 mm is analyzed using the proposed method. This example was analyzed by Karabalis & Beskos (1983), Li & Li (2002), and Rahai & Kazemi (2008). The

column is divided into two members with boundary conditions $\Delta_1 = \Delta_2 = 0$ as shown in Fig. 6-a. Cross section dimensions of each member are shown in Table 1. The equivalent moments of inertia required to formulate the flexural stiffness matrix (Eq. 25) for each member are summarized in Table 2. The critical buckling load (P_{cr}) calculated using the proposed method is compared with those obtained by Karabalis & Beskos (1983), Li & Li (2002), Rahai & Kazemi (2008), and SAP 2000 (2009) as shown in Table 3. The results show the accuracy and efficiency of the proposed method.

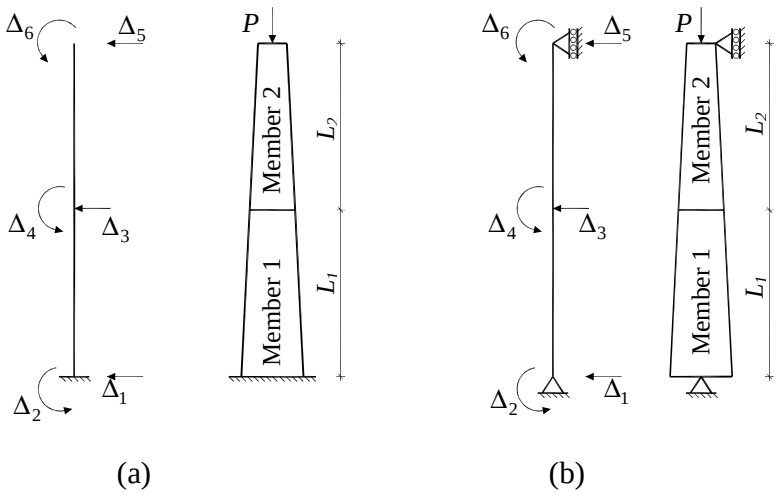

Figure 6: Verification examples: (a) example 1, (b) example 2 & 3

Table 1: Cross section dimensions (Example 1)

Member	Location	b_f (mm)	t_f (mm)	h_w (mm)	t_w (mm)
1	Start	25.4	2.032	26.416	2.54
	End	25.4	2.032	46.736	2.54
2	Start	25.4	2.032	6.096	2.54
	End	25.4	2.032	26.416	2.54

Table 2: Equivalent moments of inertia (Example 1)

Member	L_i (mm)	$I_s \times 10^2$ (mm^4)	$I_e \times 10^2$ (mm^4)	$a \times 10^2$ (mm^2)	$b \times 10^2$ (mm^2)	$I_1 \times 10^2$ (mm^4)	$I_2 \times 10^2$ (mm^4)	$I_3 \times 10^2$ (mm^4)
1	127	248.2	830.2	2.881	1.576	630.8	453.9	566.6
2	127	17.9	248.2	1.576	0.423	146	66.6	113.8

Table 3: Critical buckling load (P_{cr}) (Example 1)

Method	P_{cr}[1] (kN)
Karabalis & Beskos (1983)	241.08
Li & Li (2002)	238.04
Rahai & Kazemi (2008)	240.675
SAP 2000 (2009)	248.398
Present method	248.398

1. E = 206.85 GPa

5.2 Example 2

A simply supported linearly tapered steel column I-section , shown in Fig. 6-b, with modulus of elasticity E = 200 GPa and height L = 3657.6 mm is analyzed using the proposed method. This example was analyzed by Kaehler et al. (2011) using method of successive approximations. The column is divided into two members with boundary conditions $\Delta_1 = \Delta_5 = 0$ as shown in Fig. 6-b. Cross section dimensions of each member are shown in Table 4. The equivalent moments of inertia required to formulate the flexural stiffness matrix (Eq. 25) for each member are summarized in Table 5. The critical buckling load (P_{cr}) calculated using the proposed method is compared with those obtained by Kaehler et al. (2011) and SAP 2000 (2009) as shown in Table 6. The results show the accuracy and efficiency of the proposed method.

Table 4: Cross section dimensions (Example 2)

Member	Location	b_f (mm)	t_f (mm)	h_w (mm)	t_w (mm)
1	Start	152.4	6.35	457.2	3.175
	End	152.4	6.35	609.6	3.175
2	Start	152.4	6.35	304.8	3.175
	End	152.4	6.35	457.2	3.175

Table 5: Equivalent moments of inertia (Examples 2)

Member	L_i (mm)	$I_s \times 10^5$ (mm^4)	$I_e \times 10^5$ (mm^4)	$a \times 10^2$ (mm^2)	$b \times 10^2$ (mm^2)	$I_1 \times 10^5$ (mm^4)	$I_2 \times 10^5$ (mm^4)	$I_3 \times 10^5$ (mm^4)
1	1828.8	1293	2435	156.05	113.70	2094	1774	1983
2	1828.8	543.4	1293	113.70	73.72	1056	838.1	978.6

Table 6: Critical buckling load (P_{cr}) (Example 2)

Method	P_{cr}[1] (kN)
Kaehler et al. (2011)	17704
SAP 2000 (2009)	18093
Present method	18093

1. E = 200 GPa

5.3 Example 3

A simply supported linearly tapered steel column I-section, shown in Fig. 6-b, with modulus of elasticity E = 200 GPa and height L = 10 m is analyzed using the proposed method. This example was analyzed by Bazeos & Karabalis (2006). The column is divided into two members with boundary conditions $\Delta_1 = \Delta_5 = 0$ as shown in Fig. 6-b. Cross section dimensions of each member are shown in Table 7. The equivalent moments of inertia required to formulate the flexural stiffness matrix (Eq. 25) for each member are summarized in Table 8. The critical buckling load (P_{cr}) calculated using the proposed method is compared with those obtained by Bazeos & Karabalis (2006) and SAP 2000 (2009) as shown in Table 9. The results show the accuracy and efficiency of the proposed method.

Table 7: Cross section dimensions (Example 3)

Member	Location	b_f (mm)	t_f (mm)	h_w (mm)	t_w (mm)
1	Start	118	7.5	145	5.6
	End	118	7.5	225	5.6
2	Start	118	7.5	65	5.6
	End	118	7.5	145	5.6

Table 8: Equivalent moments of inertia (Examples 3)

Member	L_i (mm)	$I_s \times 10^4$ (mm^4)	$I_e \times 10^4$ (mm^4)	$a \times 10^2$ (mm^2)	$b \times 10^2$ (mm^2)	$I_1 \times 10^4$ (mm^4)	$I_2 \times 10^4$ (mm^4)	$I_3 \times 10^4$ (mm^4)
1	5000	1172	2924	54.078	34.237	2364	1851	2182
2	5000	246	1172	34.237	15.692	830	537	721

Table 9: Critical buckling load (P_{cr}) (Example 3)

Method	P_{cr}[1] (kN)
Bazeos & Karabalis (2006)	190
SAP 2000 (2009)	197.59
Present method	197.59

1. E = 200 GPa

5.4 Example 4

A simply supported double tapered steel column I-section, shown in Fig. 7-a, with modulus of elasticity E = 200 GPa and height L = 8 m is analyzed using the proposed method. The column is subjected to axial compression forces at the top and mid-height as shown in Fig. 7-a. The column is divided into two members with boundary conditions $\Delta_1 = \Delta_5 = 0$ as shown in Fig. 7-a. Cross section dimensions of each member are shown in Table 10. The equivalent moments of inertia required to formulate the flexural stiffness matrix (Eq. 25) for each member are summarized in Table 11. The critical buckling load (P_{cr}) calculated using the proposed method is compared with that obtained by SAP 2000 (2009) as shown in Table 12. The results show the accuracy and efficiency of the proposed method.

5.5 Example 5

A simply supported double tapered steel column I-section, shown in Fig. 7-b, with modulus of elasticity E = 200 GPa and height L = 8 m is analyzed using the proposed method. The column is subjected to axial compression force at the top as shown in Fig. 7-b. Due to symmetry, one half of the column is analyzed with boundary conditions $\Delta_2 = \Delta_3 = 0$ as shown in Fig. 7-b. Cross section dimensions of each member are shown in Table 10. The equivalent moments of inertia required to formulate the flexural stiffness matrix (Eq. 25) for each member are summarized in Table 11. The critical buckling load (P_{cr}) calculated using the proposed method is compared with that obtained by SAP 2000 (2009) as shown in Table 13. The results show the accuracy and efficiency of the proposed method.

5.6 Example 6

A simply supported double tapered, with intermediate prismatic part, steel column I-section, shown in Fig. 8, with modulus of elasticity E = 200 GPa and length L = 12 m is analyzed using the proposed method. Due to symmetry, one half of the column is analyzed with boundary conditions $\Delta_2 = \Delta_5 = 0$ as shown in Fig. 8. Cross section dimensions of each member are shown in Table 14. The equivalent moments of inertia required to formulate the flexural stiffness matrix (Eq. 25) for each member are summarized in Table 15. The critical buckling load (P_{cr}) calculated using the proposed method is compared with that obtained by SAP 2000 (2009) as shown in Table 16. The results show the accuracy and efficiency of the proposed method.

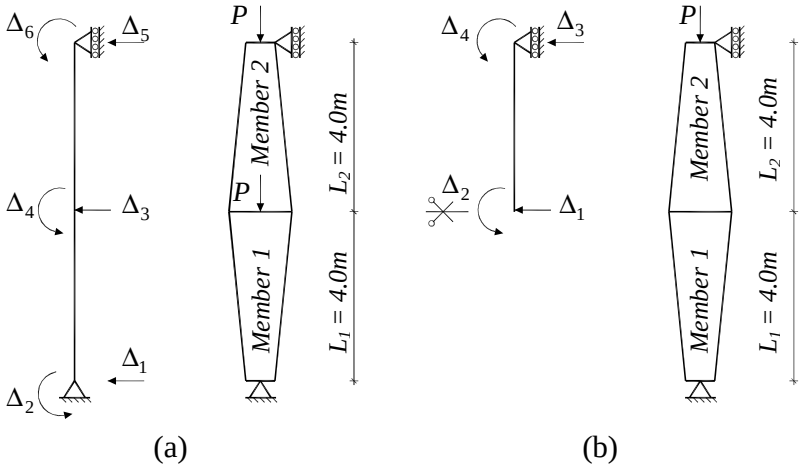

Figure 7: Verification examples: (a) example 4, (b) example 5

Table 10: Cross section dimensions (Examples 4, 5)

Member	Location	b_f (mm)	t_f (mm)	h_w (mm)	t_w (mm)
1	Start	250	10	1000	8
	End	250	10	400	8
2	Start	250	10	400	8
	End	250	10	1000	8

Table 11: Equivalent moments of inertia (Examples 4, 5)

Member	L_i (mm)	$I_s \times 10^5$ (mm^4)	$I_e \times 10^5$ (mm^4)	$a \times 10^2$ (mm^2)	$b \times 10^2$ (mm^2)	$I_1 \times 10^5$ (mm^4)	$I_2 \times 10^5$ (mm^4)	$I_3 \times 10^5$ (mm^4)
1	4000	19420	2528	159.01	440.66	4545	7007	5275
2	4000	2528	19420	440.66	159.01	12600	7007	10430

Table 12: Critical buckling load (P_{cr}) (Example 4)

Method	P_{cr}[1] (kN)
SAP 2000 (2009)	23546
Present method	23546

1. E = 200 GPa

Table 13: Critical buckling load (P_{cr}) (Example 5)

Method	P_{cr}[1] (kN)
SAP 2000 (2009)	35890
Present method	35890

1. E = 200 GPa

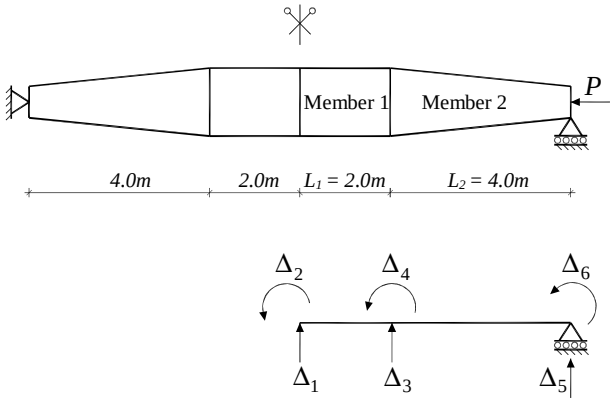

Figure 8: Verification example 6

Table 14: Cross section dimensions (Example 6)

Member	Location	b_f (mm)	t_f (mm)	h_w (mm)	t_w (mm)
1	Start	250	10	1000	8
	End	250	10	1000	8
2	Start	250	10	400	8
	End	250	10	1000	8

Table 15: Equivalent moments of inertia (Example 6)

Member	L_i (mm)	$I_s \times 10^5$ (mm^4)	$I_e \times 10^5$ (mm^4)	$a \times 10^2$ (mm^2)	$b \times 10^2$ (mm^2)	$I_1 \times 10^5$ (mm^4)	$I_2 \times 10^5$ (mm^4)	$I_3 \times 10^5$ (mm^4)	Comments
1	2000	19420	19420	440.66	440.66	19420	19420	19420	Prismatic
2	4000	2528	19420	440.66	159.01	12600	7007	10430	

Table 16: Critical buckling load (P_{cr}) (Example 6)

Method	P_{cr}[1] (kN)
SAP 2000 (2009)	21410
Present method	21400

1. E = 200 GPa

6. Inelastic Buckling Load of Tapered Column

The inelastic buckling load of a tapered column in a braced frame can be calculated following the same concept developed by Kaehler et al. (2011) in the AISC design guide for frame design using web-tapered members. The ratio of the elastic critical buckling load, P_{cr}, (calculated using the present study) to the applied axial force on the column, P_r, defines the scalar ratio, g_e.

$$g_e = \frac{P_{cr}}{P_r} \tag{34}$$

For a tapered column where the in-plane flexural buckling is the governing mode, the critical buckling strength of the column can be calculated using the equations developed by Kaehler et al. (2011):

when $\frac{QF_y}{g_e f_r} \le 2.25$

$$F_{cr} = \left[0.658^{\frac{QF_y}{g_e f_r}} \right] QF_y \tag{35}$$

when $\frac{QF_y}{g_e f_r} > 2.25$

$$F_{cr} = 0.877 g_e f_r \tag{36}$$

where F_{cr} is the nominal buckling strength, Q is the slenderness reduction factor, and f_r is the required axial stress calculated at the location of the smallest area along the column, and F_y is the yield strength.

7. Conclusions

A closed form stiffness matrix for flexural buckling analysis of web tapered steel member is developed. Only the flexural stiffness is considered: the axial and shear stiffnesses are not considered. The concept of equivalent prismatic member is developed to map a web tapered member to a prismatic one. The mapping is achieved through only three main variables, equivalent moments of inertia, calculated using closed form equations. This procedure eliminates the need for numerical methods, widely used in finite element programs, to calculate the elastic stiffness matrix of web tapered members. The proposed method is applicable for both braced and unbraced steel frames to calculate the elastic critical buckling load. This method could be applied to a wide variety of web tapered steel structures. The elastic critical buckling load of stepped column with different axial load in each segment could be determined using the proposed procedures. Other benefit of developing a closed form stiffness matrix for buckling analysis of web tapered members is its application in a computerized program to determine the elastic critical buckling load.

To demonstrate the efficiency and accuracy of the proposed method, several examples are analyzed and compared with analytical and numerical solutions available in the literature. The comparisons proved that with only two elements per member accurate result is achieved.

References

Bai R., Liu S.W., Chan S.L. (2018). "Finite-element implementation for nonlinear static and dynamic frame analysis of tapered members." *Eng Struct*, 172, 358-381.

Bazeos, N., Karabalis, D.L. (2006). "Efficient computation of buckling loads for plane steel frames with tapered members." *Engrg. Struct.*, 28 (5) 771-775.

Cook R.D., Malkus D.S., Plesha M.E. (1989). "Concepts and applications of finite element analysis." 3rd ed. John Wiley & Sons, New York.

Funk R.R., Wang, K. (1988). "Stiffness of nonprismatic member." *J. Struct. Engrg.,* ASCE, 114(2), 489-494.

Kaehler R.C., White D.W., Kim Y.D. (2011). "Frame design using web-tapered members." American Institute of Steel Construction.

Karabalis D.L, Beskos D.E. (1983). "Static, dynamic and stability analysis of structures composed of tapered beams." *Computers & Structures*, 16(6), 731–748.

Li GQ, Li JJ. (2002). "A tapered Timoshenko–Euler beam element for analysis of steel portal frames." *J Constr Steel Res*, 58 (2002) 1531–1544.

Liu S.W., Bai R., Chan S.L. (2016). “Second-order analysis of non-prismatic steel members by tapered beam–column elements.” *Structures* 6, 108–118.
McGuire W., Gallagher R.H., Ziemian R.D. (2000). “Matrix structural analysis.” 2nd ed. John Wiley & Sons, New York.
Rahai A.R., Kazemi S. (2008). “Buckling analysis of non-prismatic columns based on modified vibration modes.” *Communications in Nonlinear Science and Numerical Simulation* 13, 1721–1735.
SAP 2000, V.14. (2009). Computers and Structures, Inc., Berkeley, CA, USA.
Teh, L.H. (2001). “Cubic beam elements in practical analysis and design of steel frames.” *Eng Struct*, 23 (10), 1243-1255.
Timoshenko S.P., Gere, J.M. (1961). “Theory of elastic stability.” McGraw-Hill, New York.
Williams, F.W., Aston, G. (1989). “Exact or lower bound tapered buckling loads.” *J. Struct. Eng.*, ASCE, 115(5), 1088-1100.